Original Research Article

The Geophysical Investigation of Leachate Formation in Mgbuka Obosi, Idemili North Local Government Area of Anambra State, Nigeria

Abstract

The contamination of leachates (a polluted liquid made up of various toxic substances) from landfills is a significant environmental concern, especially in developing countries. This contaminated fluid is formed when rainwater interacts with refuse and travels through the pore spaces in soil. Constant migration of this fluid poses a significant threat to the quality of both surface and groundwater in and close to the landfill area. To address this issue, the study used both Very Low-Frequency Electromagnetic (VLF-EM) and Electric Resistivity Tomography (ERT) to locate and define the spatial distribution of the leachate plume migration pathway at Mkpuka Obosi Dumpsite in Idemili North LGA of Anambra, Nigeria. Seven profiles were surveyed for both the VLF-EM and ERT. The VLF-EM survey, with a profile length of 100 to 200m and a 10m interstation spacing, revealed the presence of a conductive pollutant (leachate plume) in the subsurface. The results from the 2D ERT survey that employed a Wenner array with a profile length of 100 to 200m and an electrode spacing of 5m, divided the subsurface into six zones with an unusually low resistivity ranging from 0-250Ωm. The leachate plumes were interpreted as the zone with the lowest resistivity of 0 to 25Ωm, having an average thickness of approximately 10m and extending beyond the probed depth of 50m. Additionally, the percentage of leachate was found to be concentrated primarily at the center of the landfill, gradually decreasing proportionally from the center. Thus, emphasizing the importance of addressing the issues in landfill management.

Keywords: Leachate, Landfill, Dumpsite, VLF-EM, ERT, Dispersive clay.

Introduction

Landfilling is a waste disposal method that involves filling up the land's depressions, such as excavation sites, valleys or erosion-affected areas, with solid wastes [1]–[3]. It can also be practiced in certain areas within a community where an unpleasant event occurred and requires covering up. This waste management technique is considered the simplest, cheapest, and most cost-effective means of waste disposal utilized in both developing and developed nations [4]–[6].

During rainfall, water penetrates through the soil pores and cells of landfills, where it interacts with decomposed solid waste consisting of organic and inorganic chemicals, biological waste, and metals, among others, to form a polluted plume known as leachate, which tends to be acidic [3], [7]. While developed countries utilize liners to prevent the liquid generated by decomposing materials from escaping, many developing nations lack the financial resources to afford such systems, resulting in the migration of leachate into the unsaturated soil zone and eventually, the groundwater [1], [9]. This poses a significant risk to the water supply; a vital resource relied upon by the community for their daily needs.

It is however imperative to address the magnitude of leachate migration to the aquifer and prioritize the identification and tracking of its pathway. Various methodologies are commonly employed to address this issue in landfill management. Thus, it is crucial to seek alternatives that minimize costs, minimize disruption to daily operations, and optimize the utilization of resources. In this regard, an effective geophysical approach can be employed to assess the extent of leachate migration within the subsurface[12].

Multiple geophysical techniques are available for this purpose, two of which are the Very Low-Frequency Electromagnetic (VLF-EM) method and the Electric Resistivity Tomography (ERT) method. The VLF-EM method relies on the utilization of remote low-frequency radio transmissions as an electromagnetic source. This technique enables the mapping of the subsurface by identifying variations in electromagnetic responses associated

with leachate migration and other geological features. On the other hand, the ERT method involves mapping the conductivity and fracture zones within the subsurface, which encompass both aquifers and contaminated areas. By obtaining a detailed understanding of the subsurface's electrical resistivity, this method provides valuable insights into leachate migration patterns.

By employing these geophysical techniques[5], [12]–[16], it is possible to assess the extent and pathways of leachate migration in a cost-effective and non-invasive manner. This approach minimizes the need for large-scale excavation, which can be both economically burdensome and disruptive to daily activities. The use of geophysical methods provides a valuable tool for landfill management and facilitates informed decision-making regarding the prevention and mitigation of environmental contamination [17].

In this study, we aim to use these methods to determine the spatial distribution of contaminated patches that have migrated within the subsurface of an Obosi landfill site in Anambra State.

Study Area

The study was conducted in Mgbuka Obosi, a location situated in Idemili North Local Government Area of Anambra State. The area is characterized by plains with elevations between 50-200m above sea level and experiences annual rainfall ranging from around 2500mm to 4000mm, with the highest precipitation occurring in April and October. The average relative humidity hovers around 80%, while it goes up to 90% during the wet season. Figure 1 displays a map of the Idemili North region, highlighting the location of Obosi.

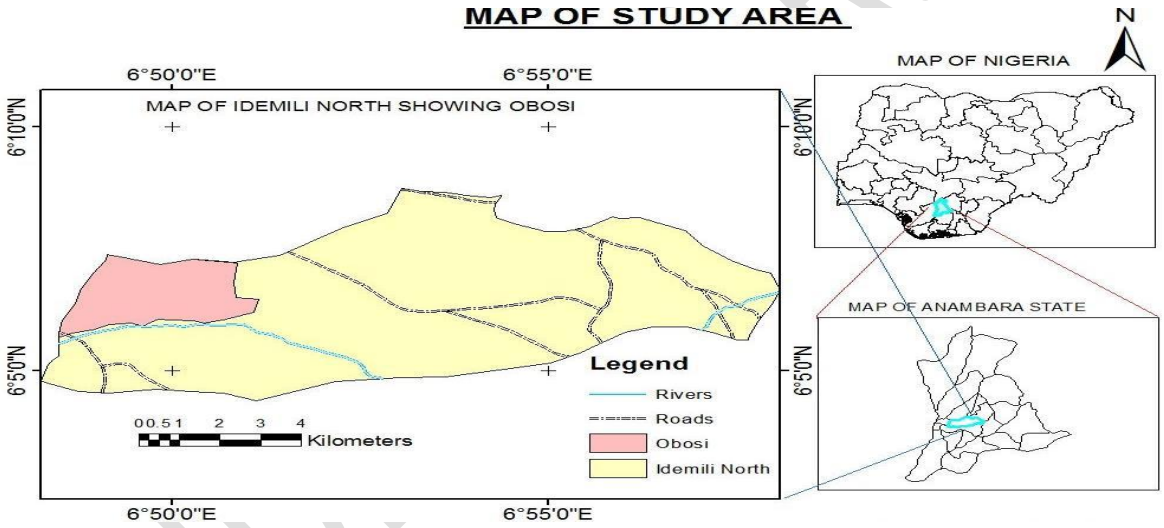

Figure 1: Map of Idemili North showing Obosi. (Source: Cartography Department of National Population Commission Anambra State, 2006)

3.1.2 The Obosi Dumpsite

The Obosi landfill site is situated between longitude 06° 47′ 59.2″ E and latitude 06° 06′ 07.8″ N, surrounded by residential structures over an area of approximately four hectares. It has been in operation in the study area for more than 50 years, and the dump comprises several categories of solid waste such as food waste, plastics, textiles, paper, e-waste, scrap metal, batteries, used tires, and used oil. Figure 2 shows a section of the Obosi dumpsite with a proliferation of different categories of solid wastes.

Figure 2: Obosi Dumpsite

Geology and Lithostratigraphic of Study Area

The study area is situated within the Anambra Sediment Basin, located in southeast Nigeria, which spans an estimated area of 40,000 km2 (ESMP, 2016), depicted in Figure 3. Its southern boundary coincides with the deltaic swamps of the Niger Delta basin, and it extends northwards beyond the Bende-Ameki Formation. Geologists believe that the basin originated simultaneously with the Abakaliki-Benue mountainous region, which underwent folding and uplifts during the Santonian era. The Anambra Basin is recognized as a significant depocentre of elastic sediments and deltaic sequences formed from the second phase of tectonic activity in the lower Benue Trough (ESMP, 2016). The geological map of the southern region of Anambra is available in Figure 3.

The groundwater reservoirs present in the soils of Anambra State exacerbate ecological challenges in the area. These soils are predominantly coastal plain sands, highly vulnerable to erosion, and contribute to severe ecological damage in the region. The geologic rocks and material beneath the unstable and poorly consolidated lateritic and acidic soils are also highly susceptible to erosion. Within the sandy components of these geologic units, enormous groundwater reservoirs known as aquifers exist that pose a threat when subjected to uncompromising loads from superimposed structures, leading to pore water pressures. Furthermore, the easily erodible lateritic and sandy soils are susceptible to damage by stormwater runoffs.

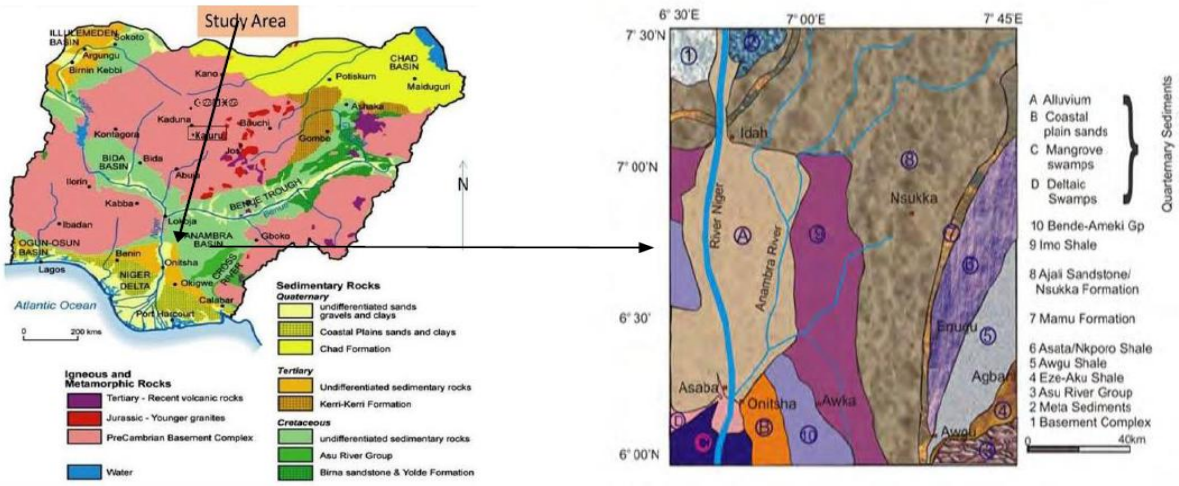

Figure 3: Geological Map of Nigeria and the Southern Anambra Basin.

Method

The VLF-EM method is a low-cost and less cumbersome geophysical technique. It primarily uses inductive primary EM waves to induce a secondary EM wave in the form of eddy currents to map shallow subsurface structural feature.

The VLF meter, ABEM WADI VLF EM, is a battery powered digital indicator that uses a transmitter operating between 15KHz and 25KHz from a powerful radio satellite to generate a time-varying very weak electromagnetic field, the primary field, which can travel very long distances penetrating the subsurface to induce eddy current, the secondary field, in the buried conductor.

The ABEM WADI VLF measures the primary field, the secondary field and the phase lag between the primary and secondary fields. When analysed, this information can be used to detect the presence of a conductor or conductive zone in the ground. For example, a phase lag of the secondary EM field relative to the primary EM field of about half a period (180^0) indicates a conductive ground. A ground with a high resistivity (poor conductor) will cause the secondary EM field to lag behind the primary field by a period of 90^0 [18]. Only the inphase and outphase components are recorded by the ABEM WADI VLF. The ratio of the real component to the imaginary component determines the degree of conductivity [19].

For the analyses of VLF-EM data, a RAMAG and KHFfilt software are used for to find the characteristic of the cross sectional depth wise of a single profile and filtering respectively.

Karous-Hjelt filters are an example of linear filters that process the real and imaginary components of the magnetic field, while Fraser filters operate on the tilt angle [20]; [21]. The ellipticity and tilt angle of the polarization ellipse are used in the calculation of the real and imaginary responses. The tilt angle (Ø) is the angle of the major axis of the ellipse, while the ellipticity (e) [21] is the ratio of the minor axis to the major axis, as described by the following equations [19].

$$Tan(2\theta) = \pm\frac{2(H_z/H_x)Cos\Delta\emptyset}{(H_z/H_x)^2} \quad (1)$$

Where $H_z$and H_x are the amplitude of the phase difference,$\Delta\emptyset = \emptyset_z - \emptyset_x$, and in which $\emptyset_z$is the phase of *Hz* and $\emptyset_x$is the phase of *Hx* and . $H_i = \left|H_z e^{i\Delta\emptyset} sin\theta + H_x Cos\theta\right|$ (2)

From the ellipticity and tilt angle the real and imaginary responses for the conductor can be calculated from the equation (5)[20], [22]:

$$Real = 100Tan\theta \quad (3)$$

$$Real\% = 100\theta(\theta - inRadian) \quad (4)$$

$$Imaginary = 100e \quad (5)$$

For this study, seven profiles with a transverse length of 200 m and a station spacing of 5 m were analysed using the ABEM WADI VLF-EM instrument. Each profile was oriented in a NW-SE direction to follow the stress formation of the study area. This was done to reduce complications due to anisotropic effects associated with the study area.

ERT Method

The 2D resistivity data were collected along the profiles using a Wenner array. The total length of the profiles and the spacing of the electrodes for this campaign are the same as those used for VLF-EM. The choice of the electrode arrays was adopted because its ability to provide an optimal depth of investigation, horizontal resolution, and data coverage[23]. The 2D data were processed and inverted using the DeproWin inversion algorithm. The algorithm calculates apparent resistivity values using a forward modelling subroutine (AGI, 2003). It generates the inverted resistivity depth image for each profile line. This is based on an iterative smoothness constrained least squares inversion algorithm[23]. In general, the program automatically creates a 2D model by dividing the subsurface into rectangular blocks [24]. The resistivity of the model blocks was iteratively adjusted to

reduce the difference between the measured and calculated apparent resistivity values. (A measure of this difference is given by the root mean square (RMS) error).

Result

Figures 4a to 4k illustrate the outcome of the VLF-EM geophysical survey, which utilized both Fraser filters for the current density data response and pseudo-sections of the Karous-Hjelt filtering to visualize the current density data against subsurface depth. The purpose of this survey was to detect the flow of leachate and map its distribution in the subsurface.

All Profiles in this section run from NW to SE and are separated by 100m except for Profile 7 that have different orientation that is based on the availability of space.

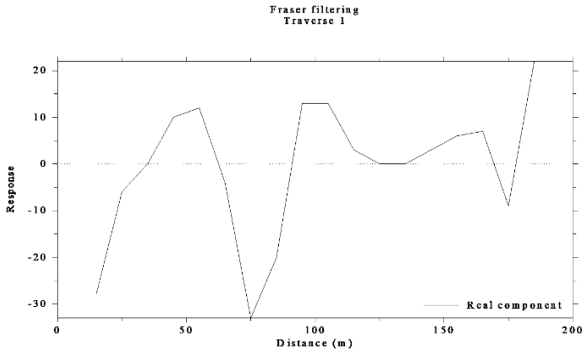

(4a)

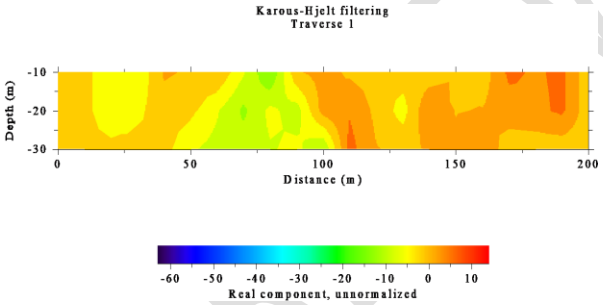

(4b)

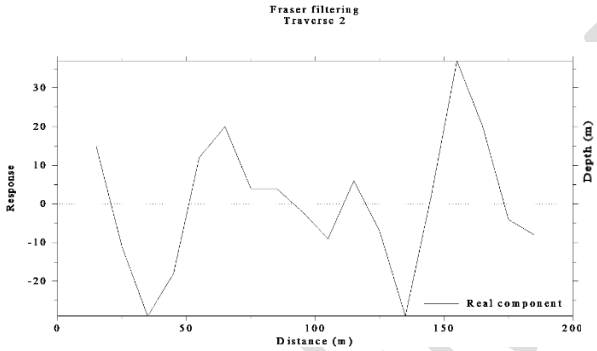

(4c)

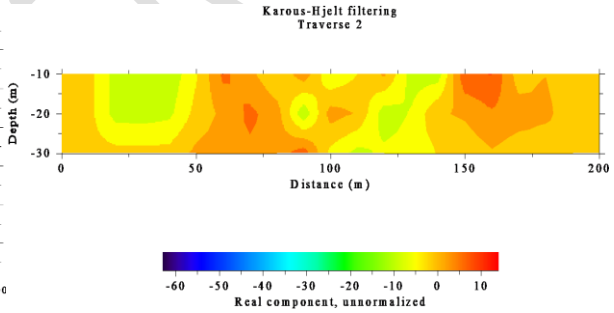

(4d)

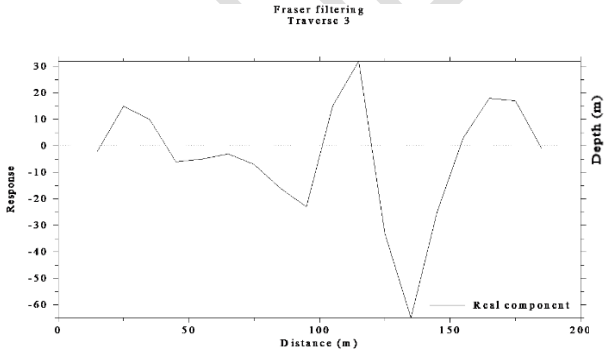

(4e)

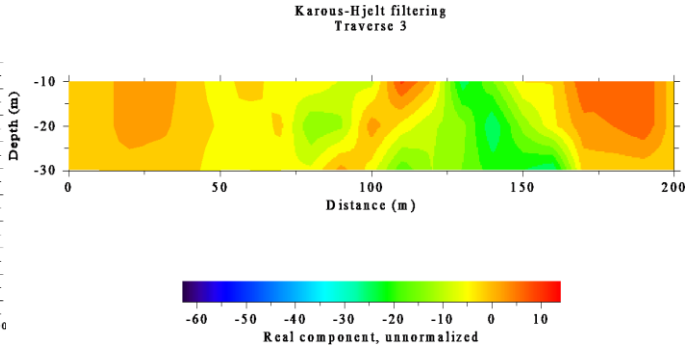

(4f)

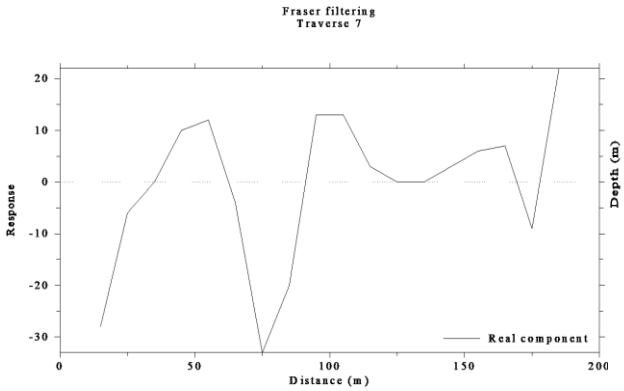

(4g)

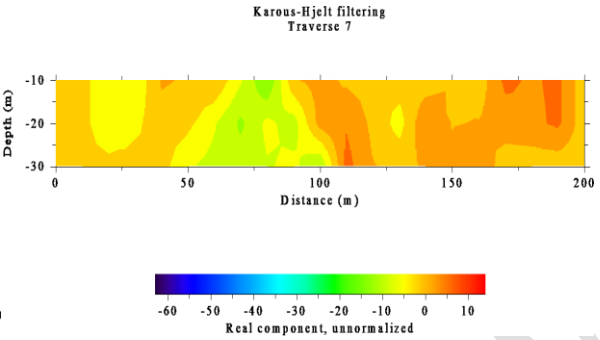

(4h)

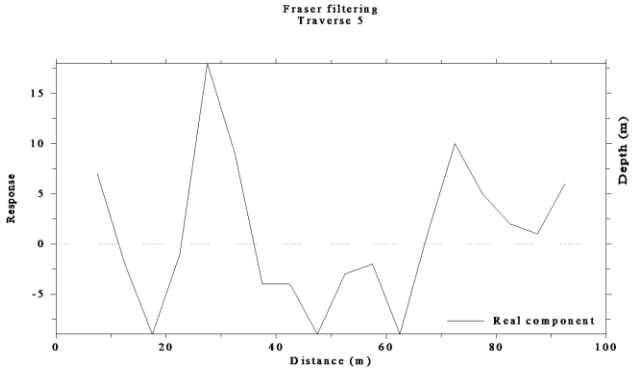

(4i)

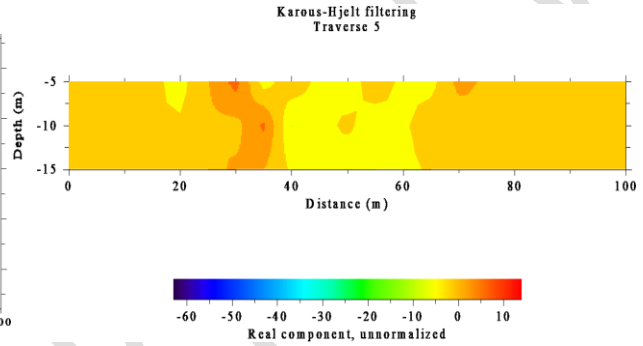

(4j)

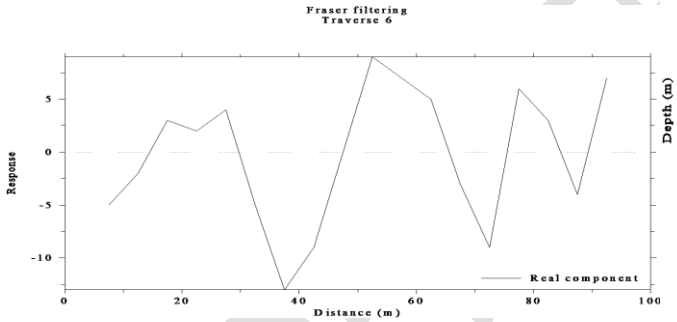

(4k)

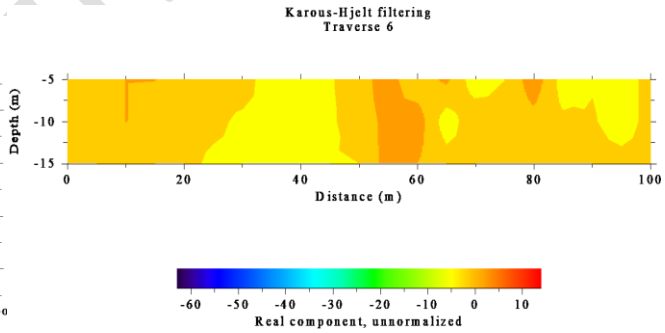

(4l)

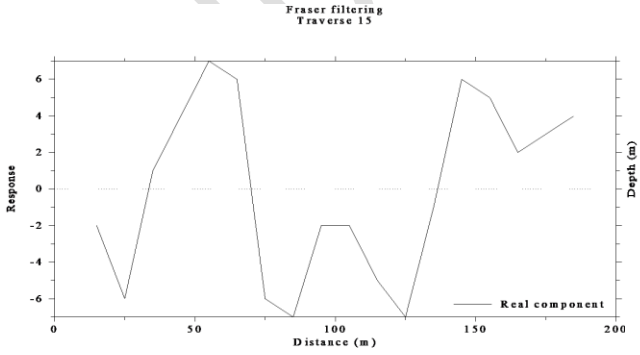

(4m)

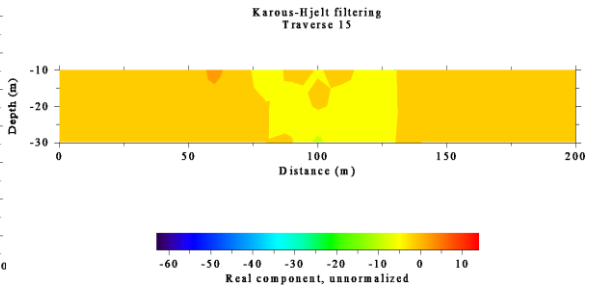

(4n)

Figure 4. Fraser and Karous Hjelt filtering.

PROFILE 1

The Fraser filtering of figure 4a, covered a distance of 200 m, while amplitude response of -35 to 20 was achieved. In the northern and central parts of the profile, a positive current amplitude response of 10 was recorded at 50m and 100m respectively. A very strong positive current anomaly response of 20 was also recorded at 180m in the southern part of the profile, indicating three areas of possible leachate accumulation/migration in Profile 1.

A depth of 30m with conductivity ranging from -60 to 10mhos was probed for the Karous-Hjelt filtration of Figure 4b. The profile shows four possible patches of leachate accumulation/migration: The first patch extends from profile distance 0 to 60m, penetrating to a depth beyond the 30m probed depth at the northern end of the profile; the second patch extends from 90m to 200m, covering 20% of the profile. Within these two patches, are two areas of high leachate accumulation ranging from 110m to 130m and extending beyond the 30m depth from the surface of the section.

PROFILE 2

Fraser filtering was applied to the profile 2, Figure 4c. A profile length of 200m was surveyed and an amplitude response ranging from -29 to 35 was detected. A positive current anomaly response of 20 was detected at the 65m mark, while a stronger positive anomaly response of 38 was found at the 170m mark, indicating the possibility of leachate formation in the subsurface.

The Karous-Hjelt filter in Figure 4d shows a sample depth of 30m. The conductivity ranges from -60 to 10mhos. The entire layout of the profile is covered with leachate, and leachate migration can be observed to penetrate beyond the 30 m depth. However, two distinct leachate accumulations can be delineated, the first extending from a profile interval of 49m to 105m and extending towards the centre of the profile. The second leachate accumulation is seen in the southern part of the profile and extends from a profile interval of 140m to 180m.

PROFILE 3

Fraser filtering was performed on profile 3, figure 4e. A total distance of 200m was surveyed and an amplitude responds of -65 to 35 were recorded. The positive amplitude response of 28 at profile distances 25m and 160m indicates possible leachate, while the highest positive amplitude response of 32, recorded at a distance of 118m.

Figure 4f shows the pseudosection of the Karous-Hjelt filtering of profile 3, Two distinct areas of high current density anomaly can be identified on this profile. The first patch ranges from a profile distance of 0m to 45m in the northern part of the profile and penetrates beyond the 30m depth from the surface, while the second patch slants and covers a distance of 35m (from 90m to 125m).

Profile 4

Figure 4g shows the Fraser filtering with a total spread of 200m and amplitudes ranging from -30 to 25. The filter suggests a possible leachate patch at a positive amplitude response of 10 at both 50m and 100m, with an additional amplitude response of 7 at 160m."

The Karous-Hjelt filter in Figure 4h surveyed a depth of 30m and a conductivity range of -60 to 10 mhos was recorded. The pseudosection shows three distinct patches of leachate generation and migration. The first patch occurs just below the surface at a distance of 40m and penetrates to a depth of 11m. The second patch forms in the center of the traverse at a distance of 85m to 125m and penetrates beyond the depth of 30m from the surface of the traverse. The third patch forms at a distance of 140m to 190m at the southern end of the traverse and penetrates beyond the depth of 30m from the surface of the traverse.

PROFILE 5

For Fraser filtering on profile 4i, a spread of 100m and an amplitude response ranging from -8 to 15 were used. Possible leachate formation can be observed at distance 4m in the northern end with an amplitude response of 7.5,

while a response of 19 is seen at a distance 15m, which is the highest current density anomaly response for this profile. Another point of interest is a response of 10 at a profile distance of 75m towards the southern end.

The Karous-Hjelt filtering was applied to profile 4j, which probed a depth of 15m, with conductivity ranging from -60 to 10mhos. The pseudosection reveals three areas containing leachate plumes. The first area ranges from 0m to 40m. Close to this area lie two patches of high conductivity, ranging from 28m to 38m and penetrating a distance beyond the 15m depth from the surface of the profile.

Profile 6

The Fraser filtering of profile 6 in figure 4k shows a total spread of 100m, with an amplitude response ranging from -8 to 15. Possible leachate formations are observed at the positive current amplitude response at the 3.5, 4.5, 10, and 6 marks, which are at distances of 16m, 25m, 58m, and 79m, respectively. The leachate formation at a distance of 58m appears to have the highest concentration of leachate accumulation.

The Karous-Hjelt filtering of profile 6 in figure 4l, probed a depth of 15m, with conductivity ranging from -60 to 10mhos. The pseudosection revealed four patches of possible leachate accumulation and migration. The first patch is located just beyond the northern end of the profile, ranging from 10m to 15m, and reaching a depth of 9m from the surface of the profile. The second patch of leachate accumulation and migration ranged from a profile distance of 55m to 61m at the center of the profile reaching a depth of 15m from the surface of the profile. The third patch that formed just beneath the surface of the profile distance 67m, penetrates a depth of 6m. The last patch formed at a distance of 80m in the southern end of the profile and penetrated a depth of 11m from the surface of the profile.

PROFILE 7 (Control Site)

Profile 7, figure 4m shows the Fraser filter with a total spread of 200m and amplitude responses ranging from -7 to 7. The filter indicates a positive current amplitude response of 6.9 at profile distances 50m, and another amplitude response of 6 at a profile distance 150m. These two responses are not strong enough to be considered leachate plume

Figure 4n, displays the Karous-Hjelt filter with a total surveyed spread of 200m and a probed depth of 30m, with conductivity ranging from -60 to 10 mhos. The pseudosection revealed only one patch of moderate conductive zone, located at a profile distance of 60m and penetrating a depth of just 10m from the profile surface.

ERT Survey

Profile 1-7 in figure 5 show the result obtained from ERT surveys at obosi dumpsite. All the pseudosection for the surveys was gotten when the apparent resistivity (Ωm) was plotted against pseudo depth (m) using a DeproWin software with an iteration of 2.4 % RMS. Depth reached for each tomogram depends on the length of the profile that was investigated. A maximum depth of 50m was obtained.

Due to anisotropic characteristic of the subsurface, the DeproWin software divides the subsurface into layers of separate colours with different resistivity. The blue colour, with low resistivity represents an area with leachate plumes, the green, an area with clay, the yellow represents sandy clay, while the red and purple colours are areas with sand and coarse sand respectively.

As in the VLF-EM analysis, areas with leachate accumulation are considered to be one with low resistivity this is because of the surface component that constitute the content of the leachate

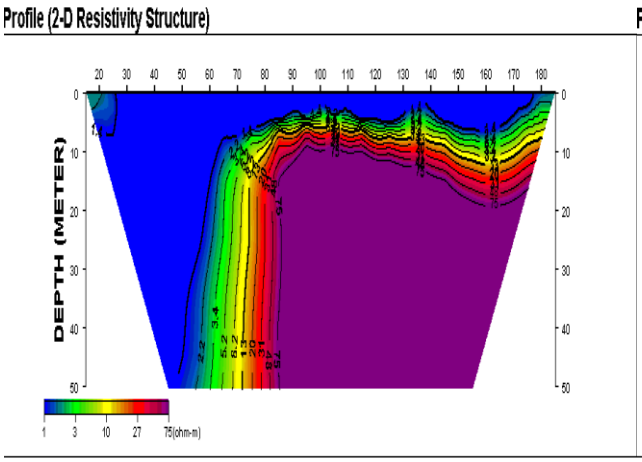

(5a)

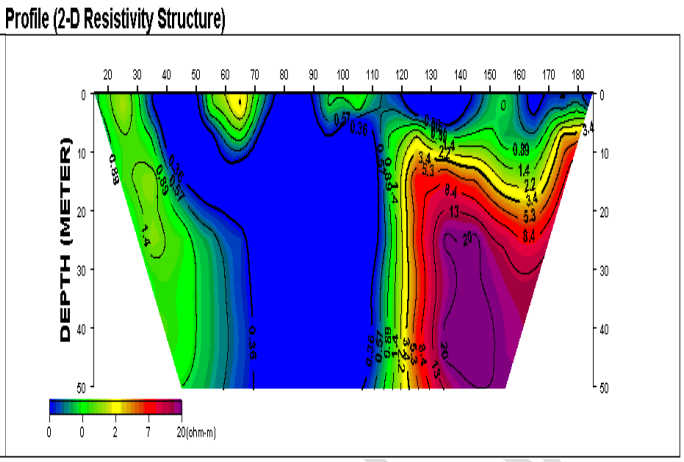

(5b)

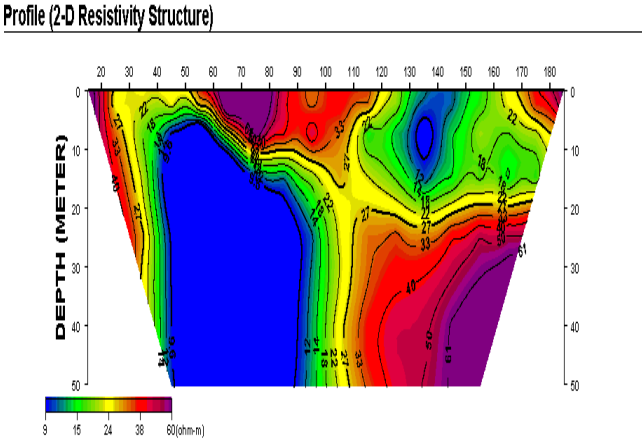

(5c)

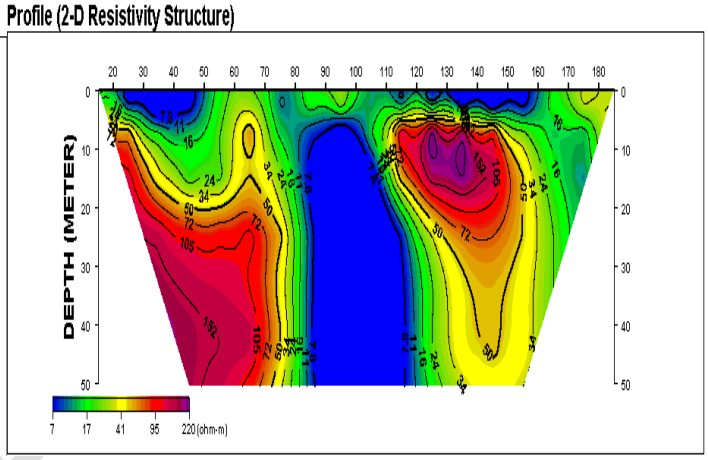

(5d)

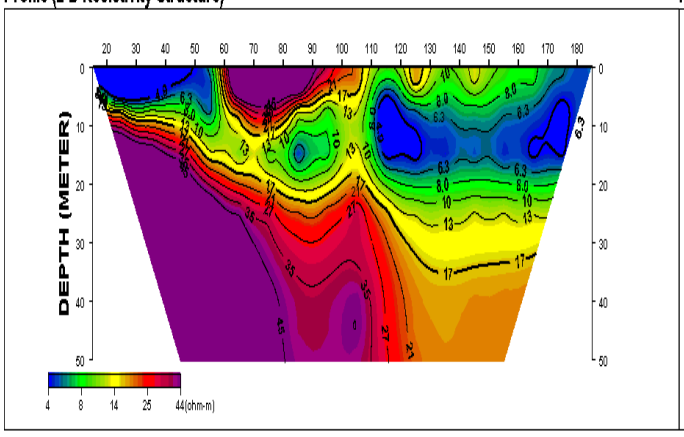

(5e)

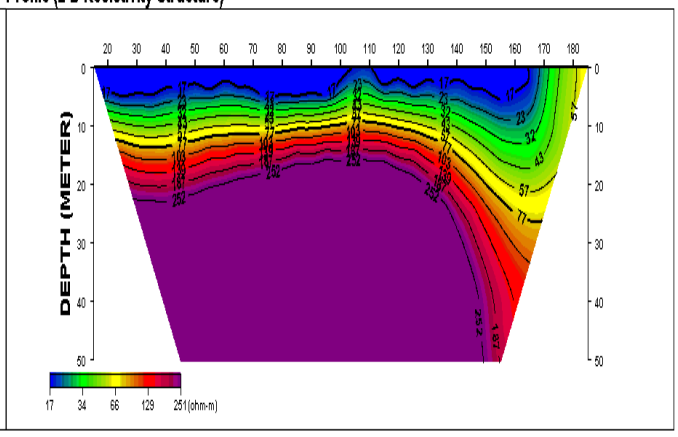

(5f)

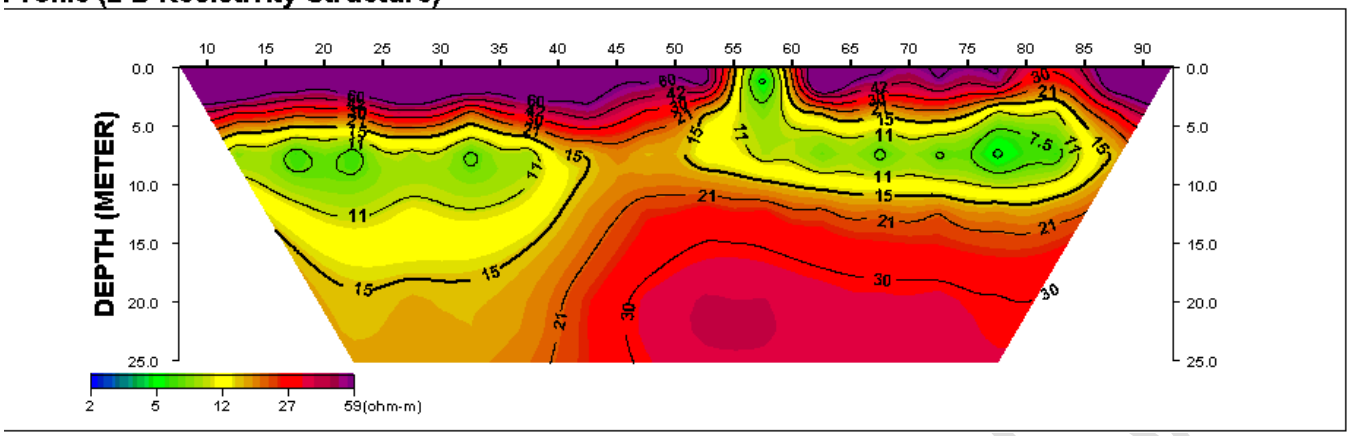

(5g)

Figure 5. 2D resistivity Images

Profile 1

The 2D ERT shown in Figure 5a has a depth of 50m and is characterized by resistivity ranging from 1-75Ωm. The saturated and unsaturated leachate has resistivity values that ranges from 1-3Ωm, and was found to be widespread across the entire length of the profile from the surface down to a depth of 50m. The clay layer under the leachate formation was around 4m thick and had resistivity values between 3-5Ωm. This clay layer cut across half of the profile length reaching a depth ranging of 50m.

Profile 2

Figure 5b is a 2D ERT modeled that surveyed a depth of 50m and records resistivity that ranges from 0-25Ωm. Five distinct resistivity structures were delineated. The resistivity of the saturated and unsaturated leachate zone varying from 0.2-0.6Ωm, cutting through the entire profile length except for few areas where they were sandwiched by clay with resistivity ranging from 0.6 - 3, the leachate penetrates a depth of 50m from the surface of Profile. The sandy clay, just besides the clayey zone, penetrates a depth of 50m from the surface of the profile with resistivity that varies from 3-6Ωm.

Profile 3

The 2D ERT model for profile 3 is shown in Figure 5c. it probed a depth of 50m with resistivity ranging from 8-60Ωm. The saturated and unsaturated leachate had resistivity values from 8-12Ωm and were found to cut across the profile length at two separate intervals: 39-95m and 135-156m, with maximum thicknesses of 45m and 49m, respectively. These layers penetrated to depths ranging from 10-50m. Additionally, a clay layer was identified with resistivity values that ranged from 14-22Ωm. This layer lies just beneath the leachate zone with a thickness of 10m penetrating beyond the 50m probed depth.

Profile 4

Figure 5d is a 2D ERT modeled section of Profile 5. a depth of 50m was probed and it is characterized by resistivity ranging from 7-220Ωm.The resistivity of the saturated and unsaturated leachate varies from 7-16Ωm, and can be located within profile length of 20-160m with maximum thickness of 30m while reaching a depth of 50m. At both sides of the leachate zone is the clay layer with resistivity that varied from 17-34Ωm. Spreading in no particular order across the entire Profile length while reaching a depth of 50m.

Profile 5

Figure 5e shows that the resistivity of the saturated and unsaturated leachate layer in the profile varies from 4-8Ωm. The layer is thickest at the southern end, where it reaches a depth of 20m and a thickness of 15m. At the northern end, the leachate layer has reached a depth of 9m and a thickness of 8m. This layer extends across the profile length in two intervals: 10-70m and 110-150m. In addition, the clay layer beneath this leachate formation has resistivity values ranging from 8-13Ωm and is around 10m thick. It is present at a depth of 0-25m and covers the entire length of the profile, forming a protective barrier against further migration of leachate.

Profile 6

In profile 6, the resistivity of both saturated and unsaturated leachate is shown in Figure 5f. These values range from 17-23Ωm and are found at a thickness of 8m, cutting through the profile length of 0-165m at a depth of 0-8m. Just below this leachate zone is a clay layer with resistivity ranging from 24-43Ωm. This layer spreads thinly across the entire profile at a depth of 0-20m. Additionally, a sandy clay layer is identified with resistivity values ranging from 57-72Ωm. This layer spreads thinly throughout the entire profile, just like the clay layer, at a depth ranging from 20-23m. Beneath the sandy clay layer is a sandy layer with resistivity values ranging from 72-181Ωm. The final layer, the coarse sand layer, has a resistivity value of 181Ωm or higher.

.Profile 7(Control Site)

The Profile, figure 5g starts with the coarse sand with a resistivity of 75Ωm, and a thickness of 3m at a depth of 5m that cuts through profile length of 0-55m and 60- 100m from the north. The 5m gap is composed of clay with a resistivity of 6-11Ωm having a thickness of 10m, surrounding the clay is the sandy clay with resistivity that varies from 12-16Ωm beneath the sandy clay is the sandy soil with a resistivity of 27-40Ωm.

There is no leachate formation in this Profile because it was carried out on the control site. This was practically done to map out the normal resistivity of the subsurface without the leachate contamination in order to give a clear description of the contaminated areas.

Distribution of Leachate Migration Areas

Figure 6 and Table 1 show different profiles of VLF-EM survey and the level of leachate migrating through them. Profiles 1 and 2, carried out at the centre of the dumpsite (the initial position of the dumpsite), show many patched areas with high conductive zones in both the Fraser and Karous-Hjelt filters. The two profiles recorded 69.3% and 53.4% of patches with a rating of very high. Profiles 3 and 4 were conducted 100m east and west from profile 1 and 2 respectively shows a moderate patch distribution with Profile 3 having a slightly higher percentage of patches (36%) than Profile 4. Profiles 5 and 6 were conducted 200m east and west of the centre of the dump near the extreme end of the dump. The conductivity of both profiles was low compared to the other four profiles. This is because the rate of migration of leachate decreases from the point of concentration of leachate formation as stated in the work of [25], [27], [30]. Profile 7 was conducted 1 km from the centre of the landfill. It is considered as the control site of the study, aiming to check and analyse the anomaly caused by the migration of the leachate. However, this profile did not record any form of leachate. It is concluded that leachate migration is only concentrated within its formation base. This may be due to the thick overburden usually encountered by migrating fluid as it travels through different rock textures [26], [31], [32].

Table 1. Percentage of the variation of leachate in the VLF-EM Karous-Hjelt filtering

Station	Area of Patches (m2)	Percentage of Patches	Rating
Profile 1	27	69.3	Very high
Profile 2	21	53.4	High

Profile 3	18	36.2	Moderate
Profile 4	9	23.1	Moderate
Profile 5	7	18.3	Low
Profile 6	8	12.8	Low
Profile 7	0.5	1.2	Very Low

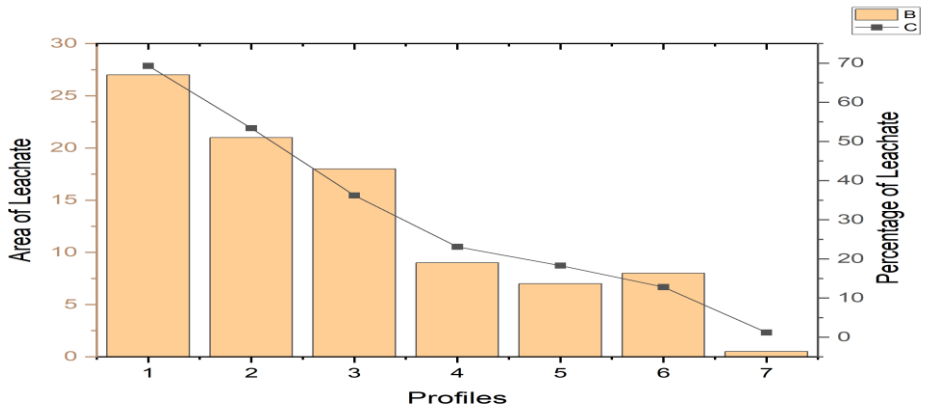

Figure 6. A graph showing the variation of leachate on profiles

According to the data presented in Table 2 and Figure 7, we can observe the patterns of leachate migration within the landfill. The table provides information on the area of the migration patches and the percentage of these patches, indicating the concentration of leachate in different areas. The graph, on the other hand, visually represents the variation of leachate along different profiles.

Analyzing Table 2, we can see that the area of the migration patches decreases as we move further from the center of the landfill. This is evident from the decreasing values in the "Area of Patches" column. Furthermore, the percentage of patches column in Table 2 provides additional insights into the distribution of leachate migration. The percentage values represent the proportion of the total area covered by the patches. As we examine the data, we can observe a similar trend to the area of patches. The percentage of patches decreases as we move away from the center of the landfill. Profiles 1 and 2 have the highest percentages of patches, indicating a higher concentration of leachate in those areas. On the other hand, Profiles 6 and 7 have the lowest percentages, suggesting a lower concentration of leachate in those regions.

To complement the information provided in Table 2, Figure 7 visually represents the variation of leachate along different profiles. The graph allows us to observe the changes in leachate concentration as we move from the center to the outer regions of the landfill. It provides a clear visual representation of the linear decrease in leachate concentration as we move further from the landfill center.

By combining the information from Table 2 and Figure 7, we can conclude that the migration of leachates within the landfill is more concentrated at the center and decreases linearly as we move further away. This understanding is crucial for effective landfill management and the prevention of contamination in surrounding areas.

Table 2. Percentage of the variation of leachate in the ERT pseudosection

Station	Area of leachates	Percentage of leachate	Rating
Profile 1	25	73.5	Very High

Profile 2	35	77.5	Very High
Profile 3	20	44	High
Profile 4	22	48.9	High
Profile 5	10	22.2	Moderate
Profile 6	8	17.7	Moderate
Profile 7	0	0	Low

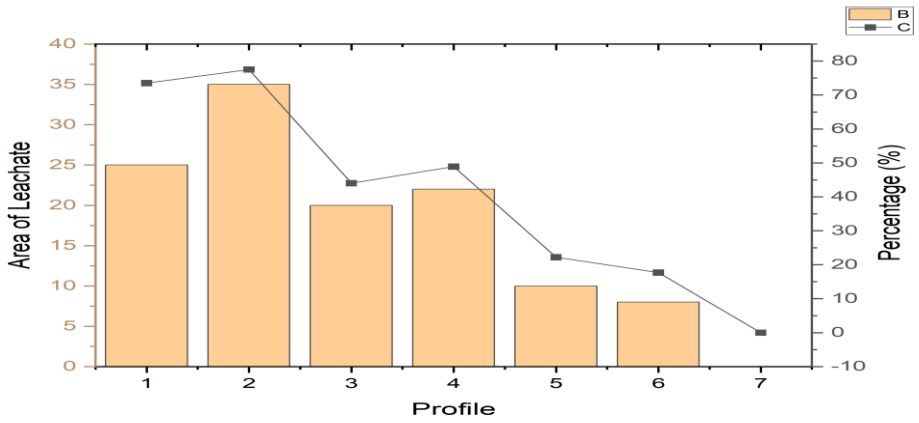

Figure 7. A graph showing the variation of leachate on profiles

Discussion

Geophysical surveys are primarily employed especially in the earth subsurface to analyse the different anomaly contained in parent rocks and to map the extents at which these anomalies have grown. This study used two different types of geophysical techniques to examine the rate at which contaminated plume from leachate have migrated in the subsurface. The results from the surveys carried out have been presented in the section above.

For easy comparison, leachates derived from the dumpsite contain dissolved ion from the interaction of water and migration through pore spaces in faults/fractures,[25]. Hence, the presence of leachate will raise the conductivity above the ground values leading to positive current density anomaly for the Fraser filtering and light pink to dark pink colours for the Karous-Hjelt filtering, [17], [26], [27].

Consequently, areas showing positive current density anomaly or light to dark pink colours along the VLF-EM profile are interpreted to be rock infiltrated by leachate. The areas with low conductive property are interpreted to be crystalline rocks, since crystalline rocks are very resistive because they lack porosity that will permit the infiltration of water or leachates [28], [29].

It could be observed generally that the subsurface is defined by low resistivity ranging from 0 -275Ωm. The contaminated plumes were interpreted as areas with very low resistivity approximately 10Ωm in the tomograms. They are occasionally sandwiched by dispersive clayey soil with an approximate resistivity of 25Ωm that were previously acting as natural liners, preventing migrating leachate. The dispersion in the clay soils are caused by the imbalance in the soil chemistry offered by the interactions of clay and leachate[33].

The control profile at an offset of 1 km showed high resistivity, which is in contrast to other profiles that showed low to moderate resistivity. This contrast can be inferred to the infiltration of leachate from the dumpsite into the subsurface, which does not occur in the control, this similar to the works of [7], [28], [31], [32], [34], [35]

Conclusion

The study was carried out to determine the extent of leachate contamination in Mgbuka Obosi dumpsites. The geophysical techniques utilized were VLF-EM and ERT. The results of the geophysical survey indicated the development of subsurface high conductivity zones for VLF-EM and very low resistivity zones for ERT within and outside the landfill boundaries. The interpretation of the VLF-EM and ERT data suggests the presence of leachate, with the models indicating that the leachate may have migrated to the aquifer of the study area. The extent of the migration may also be due to the weak and thin clay formations, which are considered to be in dispersive conduction due to their interaction of contaminated leachate. The study also shows that the contaminated plumes are moving away from the center of the dumpsite. This suggests the spatial distribution of leachate in the area.

References

[1] A. A. Ameloko and E. A. Ayolabi, "Geophysical assessment for vertical leachate migration profile and physicochemical study of groundwater around the Olusosun dumpsite Lagos, south-west Nigeria," *Appl. Water Sci.*, vol. 8, no. 5, p. 142, Aug. 2018, doi: 10.1007/s13201-018-0775-x.

[2] O. O. Ikotun and O. S. Awokola, "Investigation Of Physico-Chemical Characteristics Of Shallow Aquifer Around Dumpsites: A Case Study Of Kajola, Agbowo Dumpsites, At Ibadan, Oyo State, South Western Nigeria.," *Int. J. Eng. Res.*, vol. 1, no. 6, 2012.

[3] I. ul H. Lone, A. Kumar, F. Khan, and S. Saxena, "Evaluating the effect of landfill leachate on groun dwater quality in relation to physicochemical and bacteriological characteristics," 2012. Accessed: Mar. 26, 2023. [Online]. Available: https://www.semanticscholar.org/paper/Evaluating-the-effect-of-landfill-leachate-on-groun-Lone-Kumar/dbd91ba444443aa6a1348828048a80bbbae5f261

[4] A. Barrett and J. lawlor, "The Economics of Solid Waste Management in Ireland," *Econ. Soc. Res. Inst. ESRI Res. Ser.*, 1995.

[5] I. Ikhifa, T. Obiekezie, and A. Iyoha, "Geophysical Contribution of Using 3D View in Landfill Site," pp. 2581–7396, Jan. 2019.

[6] J. K. Nduka, F. C. Ifeanyi, and B. U. Modozie, "Risk Assessment of Heavy Metals Contamination in Surface and Underground Water Around Dumpsite in Amaenyi, Awkasouth.," *ANSP/POLY*, vol. 001, pp. 54–65, 2013.

[7] A. O. Aderemi, A. V. Oriaku, G. A. Adewumi, and A. A. Otitoloju, "Assessment of groundwater contamination by leachate near a municipal solid waste landfill," *Afr. J. Environ. Sci. Technol.*, vol. 5, no. 11, pp. 933–940, 2011, doi: 10.5897/AJEST11.272.

[9] J. L. Porsani, W. M. Filho, V. R. Elis, F. Shimeles, J. C. Dourado, and H. P. Moura, "The use of GPR and VES in delineating a contamination plume in a landfill site: a case study in SE Brazil," *J. Appl. Geophys.*, vol. 55, no. 3, pp. 199–209, Mar. 2004, doi: 10.1016/j.jappgeo.2003.11.001.

[12] T. N. Obiekezie, "Hydrocarbon exploration in Odo Field in the Niger Delta Basin Nigeria, using a three-dimensional seismic reflection survey," *Sci. Res. Essays*, vol. 9, no. 17, pp. 778–784, Sep. 2014, doi: 10.5897/SRE2013.5528.

[13] T. N. Obiekezie and E. Bassey, "Petrophysical Analysis and Volumetric Estimation of Otu Field, Niger Delta Nigeria, Using 3D Seismic and Well Log Data," *Phys. Sci. Int. J.*, vol. 6, pp. 54–65, Jan. 2015, doi: 10.9734/PSIJ/2015/15320.

[14] I. Ikhifa, M. N. Umego, T. N. Obiekezie, and G. N. Egwuonwu, "Geophysical Evaluation of a Landfill Site in Ikpoba Okhia Local Government Area, Edo State, Nigeria," *Phys. Sci. Int. J.*, pp. 1–6, Aug. 2017, doi: 10.9734/PSIJ/2017/34850.

[15] M. Umeh, T. Obiekezie, E. Anakwuba, and J. Nwosu, *ESTIMATION OF DEPTH TO BASEMENT USING SPECTRAL ANALYSIS OF GRAVITY DATA IN PARTS OF SOUTH EASTERN NIGERIA*. 2022.
[16] O. C. Obiabunmo, M. N. Umego, T. N. Obiekezie, and A. I. Chinwuko, "Application of Electrical Resistivity Method for Groundwater Exploration in Oba and Environs, Anambra State, Nigeria," *Adv. Phys. Theor. Appl.*, vol. 37, no. 0, p. 19, 2014.
[17] A. Ayad and S. Bakkali, "Analysis of the Magnetic Anomalies of Buried Archaeological Ovens of Aïn Kerouach (Morocco)," *Int. J. Geophys.*, vol. 2018, p. e9741950, Oct. 2018, doi: 10.1155/2018/9741950.
[18] G. J. Palacky, "THE AIRBORNE ELECTROMAGNETIC METHOD AS A TOOL OF GEOLOGICAL MAPPING*," *Geophys. Prospect.*, vol. 29, no. 1, pp. 60–88, Feb. 1981, doi: 10.1111/j.1365-2478.1981.tb01011.x.
[19] P. Kaikkonen and S. P. Sharma, "2-D nonlinear joint inversion of VLF and VLF-R data using simulated annealing," *J. Appl. Geophys.*, vol. 39, no. 3, pp. 155–176, Jul. 1998, doi: 10.1016/S0926-9851(98)00025-1.
[20] M. Karous and S. E. Hjelt, "LINEAR FILTERING OF VLF DIP-ANGLE MEASUREMENTS*," *Geophys. Prospect.*, vol. 31, no. 5, pp. 782–794, Oct. 1983, doi: 10.1111/j.1365-2478.1983.tb01085.x.
[21] D. C. Fraser, "Contouring of VLF-EM Data," *Geophysics*, vol. 54, pp. 245–253, 1969.
[22] R. D. Ogilvy and A. C. Lee, "INTERPRETATION OF VLF-EM IN-PHASE DATA USING CURRENT DENSITY PSEUDOSECTIONS1," *Geophys. Prospect.*, vol. 39, no. 4, pp. 567–580, May 1991, doi: 10.1111/j.1365-2478.1991.tb00328.x.
[23] M. H. Loke and R. D. Barker, "Rapid least-squares inversion of apparent resistivity pseudosections by a quasi-Newton method1," *Geophys. Prospect.*, vol. 44, no. 1, pp. 131–152, Jan. 1996, doi: 10.1111/j.1365-2478.1996.tb00142.x.
[24] M. H. Loke, J. E. Chambers, D. F. Rucker, O. Kuras, and P. B. Wilkinson, "Recent developments in the direct-current geoelectrical imaging method," *J. Appl. Geophys.*, vol. 95, pp. 135–156, Aug. 2013, doi: 10.1016/j.jappgeo.2013.02.017.
[25] Ariyo, S .O, G. O. Adeyemi, and A. O. Oyebamiji, "Electromagnetic Vlf Survey for Groundwater Development in a Contact Terrain; a Case Study of Ishara-remo, Southwestern Nigeria.," *J. Appl. Sci. Res.*, vol. 5, no. 9, pp. 1239–1246, 2009.
[26] D. O. Onwuegbuchulam, D. O. Ikoro, V. N. Nwugha, and Okereke C. N, "Application of Very Low Frequency-Electromagnetic (VLF-EM) Method to Map Fractures/Conductive Zones in Auchi South western Nigeria," *Int. J. Eng. Sci. IJES*, vol. 5, no. 5, pp. 07–13, 2013.
[27] E. R. Olafisoye, L. A. Sunmonu, T. A. Adagunodo, and O. P. Oladejo, "IMPACT ASSESSMENT OF SOLID WASTE ON GROUNDWATER: A CASE STUDY OF AARADA DUMPSITE, NIGERIA," vol. 2, no. 2, 2013.
[28] N. Abdullahi, I. Osazuwa, and S. P.O, "APPLICATION OF INTEGRATED GEOPHYSICAL TECHNIQUES IN THE INVESTIGATION OF GROUNDWATER CONTAMINATION: A CASE STUDY OF MUNICIPAL SOLID WASTE LEACHATE," vol. 4, pp. 7–25, Oct. 2011.
[29] E. C. Ramalho, A. C. Dill, and R. Rocha, "Assessment of the leachate movement in a sealed landfill using geophysical methods," *Environ. Earth Sci.*, vol. 68, no. 2, pp. 343–354, Jan. 2013, doi: 10.1007/s12665-012-1742-8.
[30] I. U. Chibuogwu and G. Z. Ugwu, "Uncovering soil piping vulnerability using direct current geophysical techniques in Awka, Anambra State, Nigeria," *Int. J. Multidiscip. Res. Growth Eval.*, vol. 4, no. 3, pp. 426–450, 2023, doi: 10.54660/.IJMRGE.2023.4.3.426-450.
[31] N. K. Abdullahi and I. B. Osazuwa, "Geophysical imaging of municipal solid waste contaminant pathways," *Environ. Earth Sci.*, vol. 62, no. 6, pp. 1173–1181, Mar. 2011, doi: 10.1007/s12665-010-0606-3.

[32] I. Ikhifa and M. Umego, "Mapping Groundwater Contamination around a Dumpsite in Benin City, Nigeria Using VLF-EM Method," *J. Geogr. Environ. Earth Sci. Int.*, vol. 4, no. 1, pp. 1–9, Jan. 2016, doi: 10.9734/JGEESI/2016/19899.
[33] S. D. Basga, D. Tsozue, J. P. Temga, J. Balna, and J. P. Nguetnkam, "Land use impact on clay dispersion/flocculation in irrigated and flooded vertisols from Northern Cameroon," *Int. Soil Water Conserv. Res.*, vol. 6, no. 3, pp. 237–244, Sep. 2018, doi: 10.1016/j.iswcr.2018.03.004.
[34] E. A. Ayolabi, A. F. Folorunso, and O. T. Kayode, "Integrated Geophysical and Geochemical Methods for Environmental Assessment of Municipal Dumpsite System," *Int. J. Geosci.*, vol. 04, no. 05, Art. no. 05, Jul. 2013, doi: 10.4236/ijg.2013.45079.
[35] W. O. Raji and T. O. Adeoye, "Geophysical mapping of contaminant leachate around a reclaimed open dumpsite," *J. King Saud Univ.-Sci.*, vol. 29, no. 3, pp. 348–359, 2017.